Automatic Modulation Classification: Investigation for Millimeter Wave Over Fiber Channels

M. Alharbi, A. Alhuseini, A. Ragheb, M. Altamimi, T. Alshawi, and S. Alshebeili, *Member, IEEE*

***Abstract*— With the rapid development of intelligent communication systems, classical problems, such as automatic modulation classification (AMC), have gained extensive research interest. This is due to the significant role that AMC plays in many civilian and military applications. In this letter, we consider AMC for millimeter wave-over-fiber (MMWoF) communication. This type of communication is of practical interest because it enables centralized analysis and processing, taking the advantages of low transmission loss of MMW signals over fiber optic channels. In this letter, we use autoencoder neural networks for automatic features extraction and classification, preceded by a pre-processing step applied to the samples of the input signal. The performance of the system under consideration has been thoroughly investigated by simulation and verified experimentally under different impairments, including fiber chromatic dispersion and amplified spontaneous emission noise. The results are presented in terms of the probability of correct classification for different values of optical signal-to-noise ratio and different lengths of fiber channels. The results from simulation are in good match to those obtained experimentally.**

***Index Terms*— Automatic modulation classification (AMC), millimeter wave over fiber (MMWoF), neural networks (NN).**

I. Introduction

IN TRADITIONAL communication systems, the modulation scheme is known to the receiver to allow correct recovery of the transmitted message signal. However, in certain applications, this knowledge is not available and needs to be determined. Examples of such applications include intelligent surveillance and electronic warfare (EW) in military fields [1], and performance monitoring in optical networks, where knowledge of the modulation scheme and other signal parameters helps in making decisions related to signal routing and power management [2]. In intelligent communication systems, where the efficient use of communication resources is a main goal, automatic modulation classification (AMC) becomes a common need [3].

Receivers with AMC processing algorithms usually perform two main operations. The first is the signal preprocessing function that estimates/extracts certain parameters of the transmitted signal (i.e. phase and carrier frequency). The second operation is the classification process. Two main approaches are considered in the literature for the modulation classification problem: the maximum likelihood (ML) and the feature based (FB) techniques. The former approach is considered an optimum solution to the AMC problem in the sense that it maximizes the average probability of correct classification (PoCC). However, this approach is computationally intensive [4]. The second AMC approach is based on extracting features from the received signal and then applying this information to a classifier. It is worthy to note that the AMC problem has been studied extensively for the wireless channel (under additive white Gaussian noise (AWGN) and fading effects); see [3]–[6] and the references therein. However, fewer attempts and demonstrations have been reported to develop AMC algorithms under optical fiber dispersion effects.

With the rise of interest in coherent optical systems, that support higher order modulation formats, i.e. high spectral efficiency, the optical modulation classification problem has seen a flux of research in recent years [7]–[13]. Various FB approaches have been proposed that take advantage of novel signal transformations to identify the different optical modulation schemes. For instance, the authors in [7] proposed a blind AMC algorithm that relies on nonlinear power transformation to classify the signals of M-ary phase-shift keying (PSK) and quadrature-amplitude modulation (QAM). Stokes space-based and higher order statistics have been employed and demonstrated for optical systems reaching more than 800 km [8]. Besides, asynchronous amplitude histograms have been employed in AMC algorithms for both direct detection [9] and coherent detection [10], some with classification pools that include up to 64QAM signals [11]. Furthermore, the cumulative distribution function (CDF) of the received signal amplitude has been utilized to differentiate QAM modulation formats in coherent optical systems [12], [13]. Alternatively, radio/millimeter wave-over-fiber (R/MMoF) system is a candidate solution for the next generation 5G and sub-terahertz communications [14]. The literature shows a limited AMC work done in this aspect. For instance, the work in [15] considered the R/MMWoF channel, but the classification pool included up to the 16QAM scheme, and only four modulation formats were included. Further, the performance was evaluated using simulations with fiber lengths not exceeding 10 km, and no experimental validation was presented.

In this letter, we study the performance of the AMC problem using autoencoder with preprocessed samples of the received signal, and under the effects of the MMWoF channel. Autoencoders consist of two main parts that work on the data

Manuscript received April 4, 2019; revised May 9, 2019; accepted May 21, 2019. Date of publication May 24, 2019; date of current version June 19, 2019. This work was supported by the Deanship of Scientific Research at King Saud University under Grant RG-1440-112.
(Corresponding author: A. Ragheb.)

M. Alharbi, A. Alhuseini, M. Altamimi, T. Alshawi, and S. Alshebeili are with the Electrical Engineering Department, King Saud University, Riyadh 11421, Saudi Arabia (e-mail: meshal.a.s.alharbi@gmail.com; aziz.alhuseini@gmail.com; mtamimi@ksu.edu.sa; talshawi@ksu.edu.sa; dsaleh@ksu.edu.sa).

A. Ragheb and S. Alshebeili are with the KACST-TIC in Radio Frequency and Photonics Center (RFTONICS), Riyadh 11421, Saudi Arabia (e-mail: aragheb@ksu.edu.sa).

Color versions of one or more of the figures in this letter are available online at http://ieeexplore.ieee.org.

Digital Object Identifier 10.1109/LPT.2019.2918924

in opposite ways. The first part encodes the large dimension representation of the data into a more compact representation with smaller dimension, in effect providing an automatic features extraction from the high dimensional data. The other part expands the small dimension representation to the original space representation, making it works as a decoder. This architecture has an advantage in that it provides automatic and optimized feature extraction directly from raw data [16].

Here, we consider a system well-suited for signal interception. The system model consists of a receiving antenna, followed by an electrical-to-optical converter for transmission over a single mode fiber to a central office. Fiber optic channel is a good candidate to transport intercepted radio and millimeter wave signals for long distances, due to fiber low transmission loss, immunity to electromagnetic interference, and low latency [14]. In this work, we consider the AMC problem for a set of modulations commonly used in wireless communication. To the best of our knowledge, this work is the first to demonstrate by simulations and experiments the performance of AMC under the effects of MMWoF channel, operating at a frequency of 28 GHz, for six modulation formats: BPSK, QPSK, 8PSK, 16QAM, 64QAM, and 256QAM. The performance is evaluated against different MMWoF channel impairments, including fiber chromatic dispersion (CD) and amplified spontaneous emission (ASE) noise. The results are presented in terms of PoCC for different values of optical signal to noise ratio (OSNR) and different lengths of fiber channel.

II. Autoencoder Classifier

The AMC algorithm of interest has two stages: features extraction and classification. Autoencoders have been recently proposed in different applications to automatically extract the features in the first stage, while a neural-network-based classifier called softmax has been used to perform the operations of the second stage [16]. The softmax classifier is a one-layer structure, with the number of neurons is equal to the number of classes (modulation formats). The softmax layer applies the so-called softmax function (normalized exponential function) to the extracted features available at the outputs of the hidden layer of autoencoder. The output from the softmax layer is a set of positive numbers which sum up to 1. These outputs can be thought of as a probability distribution, where the output of the ith neuron is the probability that the correct output is class i. Note that the neural network for each stage is first trained individually, and then a final training (tuning) is carried out on the stacked network. This form of training is known as greedy layer-wise training of deep networks [16].

For extracting meaningful features, the autoencoder undergoes a training phase. In this study, the training data is arranged in the form of a matrix, as shown in Fig. 1, where L is the number of independent realizations; each realization consists of N complex-valued samples generated from one of the six modulation schemes. The real ($\Re[.]$) and imaginary ($\Im[.]$) parts of these samples are arranged in one column, as shown in Fig. 1. This is because the available autoencoders do not deal with complex-valued inputs. The number of realizations per modulation is set to $L/6$; that is, all modulations have the same number of training data.

Realization 1	*Realization 2*	…………	*Realization L*
$\Re[sample\ 1]$	$\Re[sample\ 1]$	…	$\Re[sample\ 1]$
$\Re[sample\ 2]$	$\Re[sample\ 2]$	…	$\Re[sample\ 2]$
⋮	⋮	…	⋮
$\Re[sample\ N]$	$\Re[sample\ N]$	…	$\Re[sample\ N]$
$\Im[sample\ 1]$	$\Im[sample\ 1]$	…	$\Im[sample\ 1]$
$\Im[sample\ 2]$	$\Im[sample\ 2]$	…	$\Im[sample\ 2]$
⋮	⋮	…	⋮
$\Im[sample\ N]$	$\Im[sample\ N]$	…	$\Im[sample\ N]$

Fig. 1. Visual representation for the training matrix.

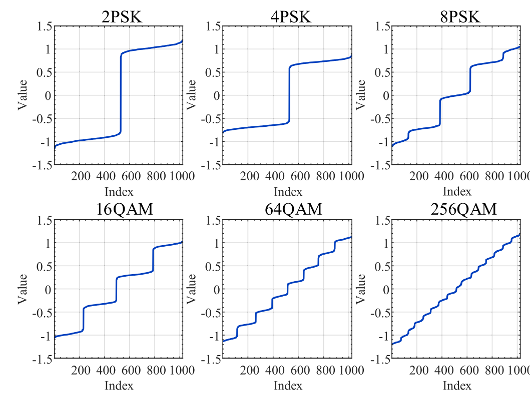

Fig. 2. Real part of sorted data at 20 dB SNR.

Once training is complete, the autoencoder is used to encode the training matrix described above by producing the hidden layer outputs. These outputs are considered features to train the softmax network. The output size of the softmax classifier is the same as the number of modulation schemes (i.e. six modulation formats in our work), and its values represent the probability that the applied input realization belongs to a specific modulation.

To form the final AMC module, we stack the encoder network of the autoencoder with the softmax classifier. This final network, consisting of one hidden layer pertaining to the autoencoder and one layer pertaining to the softmax classifier, undergoes its last training/tuning phase on labeled data. For classifying an unknown modulation, the samples of the received signal are applied to the input of the encoder so as to produce K ($<2N$) features. In this study, the value of N is 1024 and K is set to 50, based on the results of several trials. These features are then applied to the softmax layer for classification.

We propose a preprocessing step to arrange the samples of the input data using a sorting operation. Specifically, the in-phase and quadrature samples of a received signal are sorted independently and concatenated in the form of an input vector to the AMC module. The sorting could be in ascending or descending order. Fig. 2 shows the sorted real part of given realizations of modulation schemes at SNR = 20 dB. Similar results are observed for the imaginary part. The results show a distinct signature for each modulation in the form of a stair function. This function resembles the form of the CDF of a random variable, in the sense that it is monotonically increasing. That is, the sorting operation captures some statistical features of the input data, which helps to discriminate between different modulations.

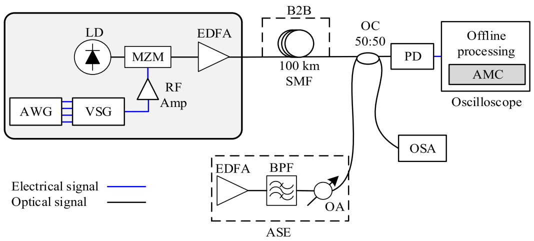

Fig. 3. Block diagram of the MMWoF system with AMC processing. AWG: arbitrary waveform generator, VSG: vector signal generator, BPF: band pass filter, OA: optical attenuator, and PD: photodetector.

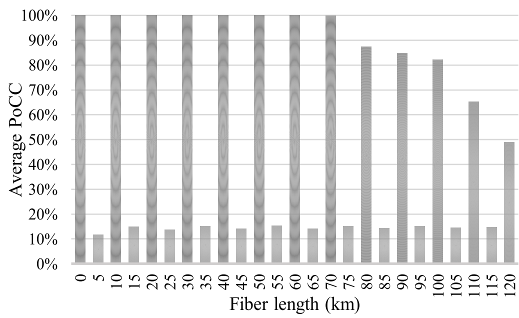

Fig. 4. Average PoCC vs. optical fiber length.

III. Simulation Results

The $VPItransmissionMaker$ 9.9 platform has been used to simulate the responses of each component, shown in the block diagram of Fig. 3. This generates the dataset necessary for the development and testing the classifier. The optimized classifier developed here is used also in Section IV to classify signals obtained from real experiments. In this setting, the length of the fiber is varied to simulate different amounts of CD. The training data matrix is structured so that it contains signals impaired by: CD (0 to 1920 ps/nm, with an increment of 160 ps/nm); OSNR (5 to 15 dB, with an increment of 5 dB); and AWGN (fixed at $E_b/N_o = 20$ dB). Additional realizations with no optical noise (representing high OSNR) were also added to the training matrix. Based on several simulations, it has been found that a training dataset in the range of 40,000 realizations, equally distributed between the six modulation formats (i.e. 128 realizations for every possible combination of the previously mentioned parameters), is sufficient to achieve good identification performance. Increasing the size of training dataset beyond that number did not contribute a noticeable improvement. It is worth noting that the training phase takes 23 minutes using a machine equipped with an Intel core i7-processor, while the testing process takes 63 μs per realization on the same machine. First, we tested the classifier with a received noiseless MMWoF signal to investigate the effect of CD. Fig. 4 shows the average PoCC results against the fiber length. It can be seen that at odd multiples of 5 km there is a huge degradation in performance, which coincides with the theoretical positions of nulls predicted by the effect of CD [17]. Because the fiber channel exhibits different characteristics for different frequencies, we expect that the performance of a classifier optimized at $f_{RF} = 28$ GHz may degrade if operated at different frequencies.

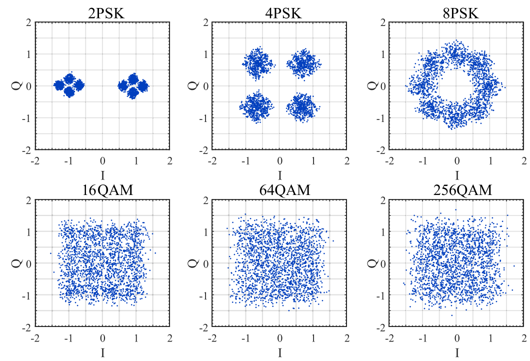

Fig. 5. Constellation diagrams under the effect of CD after 100 km.

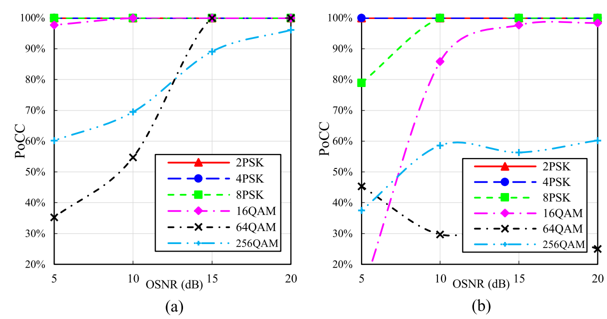

Fig. 6. Average PoCC vs. OSNR for (a) 60 km and (b) 100 km.

Additionally, Fig. 4 shows a trend in PoCC degradation not related to the fiber nulls. This results from a second CD effect on the transmitted millimeter wave signals, caused by time shifting. This degradation starts at a fiber length of 70 km, and becomes more pronounced as the fiber length increases. The amounts of CD at these lengths make the constellation symbols rotate and depart from their original positions, which results in misclassifications by the AMC algorithm. Fig. 5 shows examples of distorted signals' constellation diagrams at 100 km, owing to the lack of proper time recovery. Note that the CD fading effect can be mitigated using other MMW generation techniques such as the optical single side band (OSSB). However, the second CD effect pertaining to time shifting can't be mitigated using these optical generation techniques [17].

Fig. 6 shows the performance of proposed AMC algorithm, at 60 and 100 km fiber lengths, versus the OSNR for six different modulation schemes. At 60 km, the PoCC reaches 100% for 2/4/8PSK/16QAM and 64QAM at 10 and 15 dB OSNR, respectively. For 256QAM, the PoCC reaches 96% at 20 dB OSNR. In reference to Fig. 2, we observe that the correlation between the sorted samples of 64QAM and those of 256QAM is relatively high. This explains the behavior of the classifier shown in Fig.6 (a) at low OSNR values. At fiber length 100 km, the staircase signatures of both 64 and 256QAM diminish due to the time shifting effect of CD, and become closer in distance to the 256QAM ideal signature. This causes the 64QAM signals to be likely classified as 256QAM signals, even at high OSNR, causing the unexpected classifier behavior shown in Fig.6 (b).

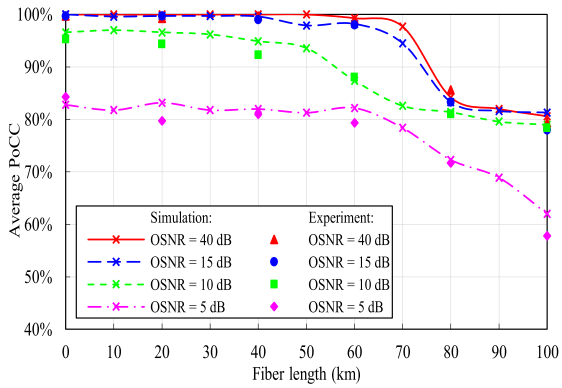

Fig. 7. Simulation vs. experiment for the MMWoF channel.

IV. Experimental Results

In this section, we present the experimental work conducted to validate the MMWoF channel simulation results. Fig. 3 shows the experimental setup of the demonstrated MMWoF system with AMC processing. A 12-GSa/s arbitrary waveform generator (Keysight M8190A) is used to generate a 1 Gbaud baseband (BB) IQ signal with various modulation formats. This includes BPSK, QPSK, 8PSK, 16QAM, 64QAM, and 256QAM. The BB signal is upconverted to 28 GHz MMW band using the Keysight E8267D, and applied to a single drive 40 GHz Mach-Zehnder modulator (MZM). The operating point of the MZM is adjusted such that a 1550 nm laser diode (LD) carries a double side band (DSB) signal (i.e. amplitude modulation). An Erbium doped fiber amplifier (EDFA) is utilized to amplify the optical modulated signal before transmission over a 100 km Corning standard single mode fiber (SSMF-28) with chromatic dispersion and polarization mode dispersion coefficients of 17 ps/nm.km and 0.2 ps/$\sqrt{km}$, respectively. The ASE noise is added to the received optical signal so as to change the OSNR values. A 50:50 optical coupler (OC) is used to combine the modulated signal with the ASE noise. The noisy optical received signal is divided into two parts: one measures the OSNR using a 0.06 nm optical spectrum analyzer (OSA); the second part is applied to a high bandwidth photodetector, which generates a 28 GHz MMW signal using the heterodyning effect. An 80-GSa/s digital storage oscilloscope (DSO) is utilized for signal analysis. The AMC technique is applied as an offline processing algorithm.

Fig. 7 shows the performance of the proposed AMC versus the fiber length, up to 100 km, at four values of OSNR of 5, 10, 15, and 40 dB, and fixed E_b/N_o at 20 dB. The experimental data here consists of 300 realizations for each OSNR and fiber length value, while the simulation results are produced according to Section III. Good agreement can be seen between the two sets of results. The classification accuracy reaches 100% at 15 and 40 dB OSNR, up to 60 km fiber length. However, the accuracy reduces to 87% and 82% at 10 dB and 5 dB OSNR, respectively. Note that at fiber lengths greater than 70 km, the performance starts to degrade due to pronounced CD effect; that is, at fiber lengths greater than 70 km the system is mainly limited by its performance against CD.

V. Conclusion

The performance of the autoencoder-based AMC algorithm was investigated, using six popular digital modulation schemes; BPSK, QPSK, 8PSK, 16QAM, 64QAM, and 256QAM, and under different impairments of MMWoF channels, including fiber CD and ASE noise. Good agreement between the simulation and experimental results was observed for different values of OSNR and different lengths of fiber. For a fiber length of 60 km, the classification accuracy is more than 98% at OSNR values greater than 10 dB. Optical single side band (OSSB) transmission right after the receiving antenna or advanced techniques at the central office could be employed to compensate for the CD fading effect. Other classifiers could also be tested to further improve the recognition accuracy.

References

[1] E. Azzouz and A. Nandi, *Automatic Modulation Recognition of Communication Signals*. Boston, MA, USA: Kluwer, 1996.

[2] J. Thrane, J. Wass, M. Piels, J. C. M. Diniz, R. Jones, and D. Zibar, "Machine learning techniques for optical performance monitoring from directly detected PDM-QAM signals," *J. Lightw. Technol.*, vol. 35, no. 4, pp. 868–875, Feb. 15, 2017.

[3] O. A. Dobre, "Signal identification for emerging intelligent radios: Classical problems and new challenges," *IEEE Instrum. Meas. Mag.*, vol. 18, no. 2, pp. 11–18, Apr. 2015.

[4] F. Hameed, O. A. Dobre, and D. Popescu, "On the likelihood-based approach to modulation classification," *IEEE Trans. Wireless Commun.*, vol. 8, no. 12, pp. 5884–5892, Dec. 2009.

[5] O. A. Dobre, M. Oner, S. Rajan, and R. Inkol, "Cyclostationarity-based robust algorithms for QAM signal identification," *IEEE Commun. Lett.*, vol. 16, no. 1, pp. 12–15, Jan. 2012.

[6] A. Hazza, M. Shoaib, S. A. Alshebeili, and A. Fahad, "An overview of feature-based methods for digital modulation classification," in *Proc. Int. Conf. Commun. Signal Process. Appl. (ICCSPA)*, Sharjah, UAE, Feb. 2013, pp. 1–6.

[7] G. Liu, R. Proietti, K. Zhang, H. Lu, and S. B. J. Yoo, "Blind modulation format identification using nonlinear power transformation," *Opt. Express*, vol. 25, no. 25, pp. 30895–30904, Dec. 2017.

[8] R. Boada, R. Borkowski, and I. T. Monroy, "Clustering algorithms for Stokes space modulation format recognition," *Opt. Express*, vol. 23, pp. 15521–15531, Jun. 2015.

[9] F. N. Khan, Y. Zhou, A. P. T. Lau, and C. Lu, "Modulation format identification in heterogeneous fiber-optic networks using artificial neural networks," *Opt. Express*, vol. 20, no. 11, pp. 12422–12431, May 2012.

[10] L. Guesmi, A. M. Ragheb, H. Fathallah, and M. Menif, "Experimental demonstration of simultaneous modulation format/symbol rate identification and optical performance monitoring for coherent optical systems," *J. Lightw. Technol.*, vol. 36, no. 11, pp. 2230–2239, Jun. 1, 2018.

[11] F. N. Khan *et al.*, "Joint OSNR monitoring and modulation format identification in digital coherent receivers using deep neural networks," *Opt. Express*, vol. 25, pp. 17767–17776, Jul. 2017.

[12] X. Lin, Y. A. Eldemerdash, O. A. Dobrem, S. Zhang, and C. Li, "Modulation classification using received signal's amplitude distribution for coherent receivers," *IEEE Photon. Technol. Lett.*, vol. 29, no. 21, pp. 1872–1875, Nov. 1, 2017.

[13] X. Lin, O. A. Dobre, T. M. N. Ngatched, Y. A. Eldemerdash, and C. Li, "Joint modulation classification and OSNR estimation enabled by support vector machine," *IEEE Photon. Technol. Lett.*, vol. 30, no. 24, pp. 2127–2130, Dec. 15, 2018.

[14] M. A. Esmail, A. Ragheb, H. Fathallah, and S. Alshebeili, "Demonstration of photonics-based switching of 5G signal over hybrid all-optical network," *IEEE Photon. Technol. Lett.*, vol. 30, no. 13, pp. 1250–1253, Jul. 1, 2018.

[15] L. Guesmi and M. Menif, "Modulation formats recognition technique using artificial neural networks for radio over fiber systems," in *Proc. Int. Conf. Transparent Opt. Netw. (ICTON)*, Budapest, Hungary, Jul. 2015, pp. 1–4.

[16] I. Goodfellow, Y. Bengio, A. Courville, and F. Bach, *Deep Learning*. Cambridge, MA, USA: MIT Press, 2017.

[17] J. Ma, J. Yu, C. Yu, X. Xin, J. Zeng, and L. Chen, "Fiber dispersion influence on transmission of the optical millimeter-waves generated using LN-MZM intensity modulation," *J. Lightw. Technol.*, vol. 25, no. 11, pp. 3244–3256, Nov. 2007.